Complete Genome Analysis of A Virulent Vibrio Scophthalmi Strain VSc190401 Isolated form Diseased Marine Fish Half-Smooth Tongue Sole, Cynoglossus Semilaevis

Zheng Zhang
Chinese Academy of Fishery Science Yellow Sea Fisheries Research Institute https://orcid.org/0000-0002-4097-8252

Yong-xiang Yu
Chinese Academy of Fishery Science Yellow Sea Fisheries Research Institute

Yin-geng Wang (wangyg@ysfri.ac.cn)
Chinese Academy of Fishery Science Yellow Sea Fisheries Research Institute

Xiao Liu
Chinese Academy of Fishery Science Yellow Sea Fisheries Research Institute

Lifang Wang
Chinese Academy of Fishery Science Yellow Sea Fisheries Research Institute

Hao Zhang
Chinese Academy of Fishery Science Yellow Sea Fisheries Research Institute

Mei-jie Liao
Chinese Academy of Fishery Science Yellow Sea Fisheries Research Institute

Bin Li
Chinese Academy of Fishery Science Yellow Sea Fisheries Research Institute

Research article

Keywords: Vibrio scophthalmi, Bacterial genome, Pathogenicity, Virulence factors, Drug resistance

Posted Date: May 13th, 2020

DOI: https://doi.org/10.21203/rs.3.rs-28392/v1

Version of Record: A version of this preprint was published on November 11th, 2020. See the published version at https://doi.org/10.1186/s12866-020-02028-7.

Abstract

Background: *Vibrio scophthalmi* is an opportunistic bacterial pathogen, which is widely distributed in marine environment. Earlier studies have suggested that it is a normal microorganism in turbot gut. However, recent studies have confirmed that this bacterial strain can cause diseases in many different marine animals. Therefore, it is necessary to investigate its whole genome for better understanding its physiological and pathogenic mechanism.

Results: In the present study, we obtained a pathogenic strain of *V. scophthalmi* from diseased half-smooth tongue sole (*Cynoglossus semilaevis*) and sequenced its whole genome. Its genome contained two circular chromosomes and two plasmids with a total size of 3,541,838 bp, which harbored 3,185 coding genes. Among these genes, 2,648, 2,298 and 1,915 genes could be found through annotation information in COG, Blast2GO and KEGG databases, respectively. Moreover, 10 genomic islands were predicted to exist in the chromosome I through IslandViewer online system. Comparison analysis in VFDB and PHI database showed that this strain had 334 potential virulence-related genes and 518 pathogen-host interaction-related genes. Although it contained genes related to four secretion systems of T1SS, T2SS, T4SS and T6SS, there was only one complete T2SS secretion system. Based on CARD database blast results, 180 drug resistance genes belonging to 27 antibiotic resistance categories were found in the whole genome of such strain. However, there were many differences between the phenotype and genotype of drug resistance.

Conclusions: Based on the whole genome analysis, the pathogenic *V. scophthalmi* strain contained many types of genes related to pathogenicity and drug resistance. Moreover, it showed inconsistency between phenotype and genotype on drug resistance. These results suggested that the physiological mechanism might be complicated.

1 Introduction

Vibrio scophthalmi was first isolated from larval turbot (*Scophthalmus maximus*) intestine by Spanish scientists in 1997 and identified as a new species of Vibrio genus [1]. In terms of phylogenetic status, this bacterium shares very high gene sequence similarity and amino acid identity with *Vibrio ichthyoenteri* [2]. Moreover, they also have similar physiological and biochemical characteristics [3]. *V. ichthyoenteri* is considered as a causative agent of Japanese flounder intestinal disease (*Paralichthys olivaceus*). Earlier studies have suggested that *V. scophthalmi* is a type of common organism colonized in turbot (*Scophthalmus maximus*) gut, which is not pathogenic and has certain host specificity for turbot [4]. Subsequently, this bacterium is successively isolated from diseased *Paralichthys olivaceus* [5], *Paralichthys dentatus* [6], *Dentex dentex* [7], *Ruditapes philippinarum* [8] and *Thunnus maccoyii* [9], supporting its pathogenicity to aquatic animals.

Current studies have proved that *V. scophthalmi* is an opportunistic pathogen [5], and it generally does not cause diseases when it is in the intestine of healthy fish. However, when the fish are subjected to

environmental stress and their immunity is weakened, they are easily infected by this bacterial strain, leading to disease or death. For example, if water temperature rises to 20℃, eel (*Anguilla japonica*) is easy to be infected by *V. scophthalmi*, which results in symptoms of severe enteritis and ascites, leading to high mortality [10]. *V. scophthalmi* can be as secondary agent to significantly increase the mortality of diseased fish after the infections of other pathogens [5]. Scientists have confirmed that *V. scophthalmi* is one of main pathogenic bacteria for Japanese flounder (*P. olivaceus*) cultured in Jeju area of Korean [11]. It is also a major pathogen of cultured turbot in China [12]. The typical symptoms of *V. scophthalmi*-infected fish include body surface blackening, ascites, enteritis and internal organ hyperaemia [5, 13], leading to 30–90% mortality of infected fish and huge economic losses.

It is generally believed that extracellular substances, including proteases and exotoxins, are the key virulence factors for most pathogenic Vibrio bacteria [14]. However, the pathogenic mechanism of *V. scophthalmi* still remains largely unexplored until now. Previous studies have confirmed that the extracellular products of *V. scophthalmi* show a variety of protease activities, such as naphthol-AS-BI-phosphohydrolase, lipase, gelatinase and leucine arylamidase [15], while no hemolytic activity or cytotoxic effect has been reported. In addition, some studies have shown that *V. scophthalmi* exhibits resistance to a variety of antibiotics [16, 17].

In the present study, a strain of *V. scophthalmi* was isolated from diseased half-smooth tongue sole (*Cynoglossus semilaevis*), and its pathogenicity to fish was verified by artificial infection experiment. Subsequently, the whole genome of this strain was sequenced and analyzed in detail. Collectively, our findings provided valuable insights into molecular mechanisms underlying the pathogenicity of *V. scophthalmi* and drug resistance.

2 Materials And Methods

2.1 The strain

V. scophthalmi strain VSc190401 was isolated from the liver of diseased half-smooth tongue sole (*Cynoglossus semilaevis*) cultured in an indoor farm. The symptoms of the diseased fish were hydrops in abdomen and intestine, as well as enteritis.

The isolated strain was purified on TSB medium for three times. The purified strain was used to prepare the living bacterial suspension at a density of 1.0×10^6 CFU/mL. The strain pathogenicity was determined through artificial challenge experiment by intraperitoneal injection. Half-smooth tongue sole and turbot with an average body weight of 50 g were selected as the experimental animals. The injection dose was 0.1 mL bacterial suspension per 50 g body weight. During the experiment, the tank was continuously air-inflated, the water was changed by 30% every day, and fish were fed once a day. The water temperature was maintained at 20 ± 1℃.

When the experimental fish developed symptoms, the dominant bacteria were isolated from the lesions, followed by purification and identification. After the isolated strain was identified as *V. scophthalmi* strain, its whole genome was sequenced on the Illumina HiSeq X platform. Meanwhile, the antibiotic resistance phenotype of this strain was detected using Kirby-Bauer disk diffusion method. A total of 38 antibiotics were tested.

2.2 Genomic DNA extraction, sequencing and assembly

Genomic DNA of *V. scophthalmi* strain VSc190401 was extracted using Wizard® genomic DNA purification kit (Promega Biotechnology Co., Ltd., Beijing, China). The quality of extracted DNA was tested using Qubit fluorometer (Thermo Fisher Scientific, Waltham, MA, USA) and Nanodrop spectrophotometer (Thermo Fisher Scientific, Waltham, MA, USA). The purified genomic DNA was quantitatively analyzed by TBS-380 fluorometer (Turner BioSystems Inc., Sunnyvale, CA, USA). Qualified genomic DNA was cut into > 10-kb fragments via G-tubes (Covaris Inc., Woburn, MA, USA) and used to construct SMARTbell DNA database after terminal repair. Genome sequencing was conducted by Majorbio Biotechnology Co., Ltd. (Shanghai, China) using the Illumina HiSeq X sequencer. The obtained SMRT original sequence data were de novo assembled by hierarchical genomic assembly process (HGAP), and the quality of newly assembled genome was corrected and verified by overlap layout consensus (OLC) and Quiver consensus algorithm to obtain the whole genome [18, 19].

2.3 Genome component analysis and functional annotation

Glimmer software was used to predict the coding sequences (CDSs) in the genome. RepeatMasker software was used to predict tandem repeat sequences [20]. The rRNAs and tRNAs belonging to non-coding RNAs were predicted by rRNAmmer software [21]and tRNAscan software [22], respectively. Furthermore, different databases, such as Gene Ontology (GO), Kyoto Encyclopedia of Genes and Genomes (KEGG), Cluster of Orthologous Groups (COG), Non-Redundant Protein Sequence Database in NCBI (NR), UniProt/Swiss-Prot, Pfam, Virulence Factors of Pathogenic Bacteria (VFDB), Pathogen Host Interactions (PHI) and the Comprehensive Antibiotic Research Database (CARD), were used to annotate the functions of coding genes. Finally, the genome circle map was drawn and annotated using the Circos software (http://circos.ca/). The genomic islands were predicted through IslandViewer online system (http://www.pathogenomics.sfu.ca/islandviewer/upload/).

2.4 Phylogenetic analysis

The complete reference genome sequences were downloaded from the NCBI database, and comparative analysis was performed based on the average nucleotide identity (ANI) value. The bacterial strains of the reference genome were as follows: *V. scophthalmi* VS-12, *V. scophthalmi* VS-05, *V. cholerae* RFB05, *V. anguillarum* ATCC-68554, *V. rotiferianus* CAIM 577, *V. harveyi* ATCC 33843, *V. parahaemolyticus* FORC_008 and *V. vulnificus* ATCC 27562.

3 Results And Discussion

3.1 The pathogenicity of strain VSc190401

The diseased half-smooth tongue sole naturally infected by strain VSc190401 showed an apparent abdominal lump (Fig. 1A). After dissection, effusion flowed out from the abdominal cavity. The internal organs exhibited serious hyperemia, and the intestinal tract became thin and transparent, which was filled with a large amount of effusion and white pus (Fig. 1B). The mortality rate of this case was more than 40%.

The half-smooth tongue sole artificially infected with strain VSc190401 also showed the same symptoms as the naturally infected fish, such as effusion in the abdominal cavity, internal organ hyperemia, and thin and transparent intestine. The artificially infected turbot did not appear abdominal lump, while the organ hyperemia and intestinal inflammation were observed. Artificial infection confirmed that the *V. scophthalmi* strain VSc190401 had a strong pathogenicity to fish.

3.2 Genomic information of strain VSc190401

After assembly, the size of the whole genome of *V. scophthalmi* strain VSc190401 was 3,541,838 bp, including two circular chromosomes (Chr I 3,286,294 bp and Chr II 202,664 bp) with approximate GC content of 45.00% and 45.37%, respectively, and two plasmids (plasmid I 24,538 and plasmid II 28,342 bp) with approximate GC content of 43.32% and 43.41%, respectively. The strain contained 3,185 coding genes, among which Chr I consisted of 2,943 CDSs, 104 tRNA genes and 37 rRNA genes. Chr II contained 188 CDSs. Plasmid I contained 32 CDSs, and plasmid II contained 22 CDSs. Figure 2 shows the genome information.

Note The outermost circle is the identification of genome size. The second and the third circle are the CDSs on the positive and negative strands, respectively, and different colors indicate the different functional annotations of CDSs in the COG database. The fourth circle is rRNA and tRNA. The fifth circle is the GC content, the red part outside indicates that the GC content of the region is higher than the average GC content of the whole genome, the blue part inward indicates that the GC content of the region is lower than the average GC content of the whole genome, and the higher peak value means the greater difference from the average GC content. The innermost circle is the GC-Skew value, and its algorithm is, which can assist to determine the leading strand and lagging strand. In general, the leading strand GC-skew > 0 and the lagging strand GC-skew < 0. The green part outside means GC-skew > 0, the orange part inward means GC-skew < 0, and the higher peak value means larger value. The legend circle1 is the functional classification in COG database, and the legend circle2 is different RNA classification.

3.3 Phylogenetic analyses

ANI analysis showed that *V. scophthalmi* strain VSc190401 was clustered with *V. scophthalmi* VS-12 and VS-05 in the whole genome of eight selected strains, and there were some genetic differences (Fig. 3). The annotation information in NCBI database indicated that *V. scophthalmi* VS-12 and VS-05 strains were all isolated from Japanese flounder cultured in Korea, containing three and two plasmids in addition to two chromatins, respectively. Based on the ANI analysis, the whole genome of *V. scophthalmi* strain

VSc190401 was found to be genetically different compared with Korean isolate strains VS-12 and VS-05, suggesting that there were some differences in host diversity or pathogenicity between Chinese and Korean isolates.

3.4 Functional annotation

COG annotation results showed that 2,648 genes were annotated into 22 types of genes, accounting for 83.14% of total genes in *V. scophthalmi* strain VSc190401. The number of each type of gene was as follows: one A-type gene (RNA processing and modification), two B-type genes (chromatin structure and dynamics), 138 C-type genes (energy production and conversion), 36 D-type genes (cell cycle control, cell division, chromosome partitioning), 199 E-type genes (amino acid transport and metabolism), 68 F-type genes (nucleotide transport and metabolism), 128 G-type genes (carbohydrate transport and metabolism), 104 H-type genes (coenzyme transport and metabolism), 59 I-type genes (lipid transport and metabolism), 167 J-type genes (translation, ribosomal structure and biogenesis), 135 K-type genes (transcription), 192 L-type genes (replication, recombination and repair), 161 M-type genes (cell wall/membrane/envelope biogenesis), 53 N-type genes (cell motility), 118 O-type genes (posttranslational modification, protein turnover, chaperones), 147 P-type genes (inorganic ion transport and metabolism), 28 Q-type genes (secondary metabolites biosynthesis, transport and catabolism), 687 S-type genes (function unknown), 140 T-type genes (signal transduction mechanisms), 99 U-type genes (intracellular trafficking, secretion, and vesicular transport), and 41 V-type genes (defense mechanisms) (Fig. 4). Supplementary Table 1 lists all COG functional annotation information.

The functional annotation results in GO database showed that 2,298 genes were annotated into three types of genes, which accounted for 72.15% of total genes of *V. scophthalmi* strain VSc190401. Among them, 1,327 genes were related to cellular component, 1,850 genes were related to molecular function, and 1,795 were related to biological process. The GO terms with the highest numbers of genes in the classification of biological process were oxidation-reduction process (174 genes, 5.46%) and regulation of transcription/DNA-templated (141 genes, 4.43%). The GO terms with the highest numbers of genes in the classification of cellular component were integral component of membrane (641 genes, 20.13%), cytoplasm (336 genes, 10.55%) and plasma membrane (91 genes, 2.86%). The GO terms with the highest numbers of genes in the classification of molecular function were ATP binding (281 genes, 8.82%), DNA binding (244, 7.66%), metal ion binding (127 genes, 3.99%), and transcription factor activity/sequence-specific DNA binding (82 genes, 2.57%). The more information were showed in Fig. 5. Supplementary Table 2 lists all GO functional annotation information.

The results of KEGG pathway analysis showed that 1,915 genes were annotated into 196 known metabolic pathways. The metabolic pathway with the largest number of genes was the biosynthesis of amino acids, containing 106 genes, followed by two-component system (96 genes), carbon metabolism (83 genes), ABC transporters (81 genes) and purine metabolism (65 genes). Cluster analysis showed that 196 metabolic pathways were categorized into six classifications of cellular processes, metabolism, human diseases, genetic information processing, organismal systems and environmental information

processing, and the numbers of genes in these six classifications were 235, 1348, 112, 219, 47 and 268, respectively (Fig. 6). The 235 genes in the classification of cellular processes could be divided into four categories, and most of them were clustered into cell motility (74 genes) and cellular community-prokaryotes (135 genes). The 1,348 genes in the classification of metabolism were divided into 12 categories. The categories with the largest gene number included global and overview maps (242 genes), carbohydrate metabolism (256 genes), amino acid metabolism (202 genes) and metabolism of cofactors and vitamins (149). The 112 genes in the classification of human diseases were clustered into 10 categories, and the categories with the largest gene number were drug resistance: antimicrobial (37 genes), and infectious diseases: bacterial (27 genes) and neurodegenerative diseases (13 genes). The 219 genes in the classification of genetic information processing were clustered into four categories. The categories with the largest gene number were translation (79 genes), replication and repair (90 genes) and folding, sorting and degradation (46 genes). The 47 genes in the classification of organismal systems were divided into eight categories. Among them, the top three categories with the largest gene number were immune system (10 genes), aging (11 genes), endocrine system (nine genes) and environmental adaptation (seven genes). The environmental information was divided into two categories, including signal transduction (115 genes) and membrane transport (153 genes). Supplementary Table 3 shows all KEGG pathway annotation information.

Through the IslandViewer online system, 10 genomic islands were predicted to be contained in the whole genome of the strain Vsc190401. They were all located on chromosome I. The longest genomic island was 34,105 bp, and the shortest one was 7,883 bp. Supplementary Table 4 and Supplementary Fig. 2 illustrate their detailed information.

3.5 Prediction of virulence genes of the strain VSc190401

To date, there are few studies on virulence factors of *V. scophthalmi*, and no specific virulence genes have been reported. A total of 334 potential virulence genes were predicted in the whole genome of the strain VSc190401. Moreover, 175 genes had annotation information in VFDB databases, including 107 offensive virulence genes, 31 defensive virulence genes, seven virulence-associated regulation genes and 30 non-specific virulence genes (Table 1). Supplementary Table 5 shows the detailed information.

Table 1
The annotation of virulence factors of the strain VSc190401 in VFDB databases

Virulence primary categories	Virulence Secondary categories	Gene numbers
Offensive virulence factors	Toxin	2
Offensive virulence factors	Secretion system	13
Offensive virulence factors	Adherence	81
Offensive virulence factors	Invasion	11
Defensive virulence factors	Cellular metabolism	1
Defensive virulence factors	Antiphagocytosis	21
Defensive virulence factors	Stress protein	9
Regulation of virulence-associated genes	Regulation	7
Nonspecific virulence factor	Iron uptake system	30

Among the offensive virulence genes, there were 81 genes related to adhesion, including flagella and pilus formation or motility exercise-related genes, such as *Flg*, *Fle*, *Flh*, *Fli*, *Tcp*, *PilB/D/G/H/R/T/U*, accessory colonization factor *AcfB/D* [23], adhesion proteins, *Lap*, *OmpU* [24] and so on. The results of comparative analysis to NR database showed that the coverage of coding protein sequences was 96.44%-100%, and the identity was 65.8%-100%. There were 11 genes related to invasion, including flagella and T4SS genes. The coverage of their coding proteins was 56.14%-100%, and the identity was 50%-100% in NR database. Moreover, 13 genes were related to secretion systems. Their sequence information was all similar to T3SS, T4SS and T6SS of Gram-negative bacteria. The coverage of their coding proteins was 91.84%-100%, and the identity was 56.7%-100%. Two toxin genes were similar to *Cya* gene, the coding proteins of which were suspected as calmodulin-sensitive adenylate cyclase-haemolysin bifunctional protein [25]. The identity of their coding proteins was 98%-99.7%.

The defensive virulence genes included 21 antiphagocytosis-related genes, nine stress protein-related genes and one cellular metabolism-related gene. The antiphagocytosis-related genes included two categories of capsule genes (*Cpa*, *Cps*) [26, 27] and alginate genes (*algB/Q/U/R/Z*, *MucA*) [28, 29]. The identity of their coding proteins was 85.6%-100%. The stress protein-related genes included superoxide dismutase enzyme gene (*sodB*), ATP-binding cassette transporter gene (*MntABC*), DNA repair protein gene (*RecN*) and respiratory metabolism gene (*ClpCP*) [30]. The identity of protein sequence was 99%-100%. The cellular metabolism-related genes were isocitratelyase coding gene fragments, with a coverage of 100% and an identity of 100%.

Among the non-specific virulence genes, the most were ATP-binding cassette transporter genes (20 genes, 98.4%-100% protein sequence identity) and bacitracin-related genes (six genes, 90%-100% protein

sequence identity). Moreover, iron uptake system-related genes, such as *FbpABC* and *FeoAB* (99.4%-100% protein sequence identity), were also found [31, 32].

The virulence-associated regulation genes contained two types of genes, *RelA* and *PhoP*. NR database comparative analysis results showed that the coverage of coding protein sequences was 100%, and their identity was 88.4%-100%. Other studies have confirmed that *RelA* and *Phop* gene regulate the synthesis of bacterial virulence factors as well as their primary and secondary metabolites, thus affecting the bacterial pathogenicity [33, 34]. In addition, the virulence-related gene sequences of *ompA* (identity 90%-100%), hemolysin (identity 96.7%-100%), beta-hemolysin/cytolysin (identity 98.2%-100%), enterobactin (identity 99.8%-100%), and T2SS (identity 97.2%-100%) were also found in the whole genome of the strain VSc190401.

Further analysis showed that the strain VSc190401 contained 36 secretion system-related genes, including one type I, 11 type II, six type IV, four type VI, 11 Sec-SRP pathway and three twin arginine targeting (Tat) pathway. The analysis results also indicated that the strain VSc190401 only had complete type II secretion system (the detailed information was shown in Supplementary Fig. 2). This finding suggested that the type II secretion system was probably the only one product export pathway.

3.6 The drug resistance phenotype and genotype analysis of the strain VSc190401

A total of 38 antibiotics belonging to 10 categories were selected to test the antimicrobial phenotype of strain VSc190401 through Kirby-Bauer disk diffusion method. The antibiotics of 10 categories were β-lactam, aminoglycosides, macrolides, tetracyclines, polypeptides, quinolones, sulfonamides, nitrofurans, amphenicols and others. The results showed that the strain VSc190401 was resistant to all aminoglycosides (including neomycin, streptomycin, kanamycin, gentamicin, amikacin), macrolides (including erythromycin, azithromycin, clarithromycin, acetylspiramycin) and amphenicols (including chloramphenicol and florfenicol). It was sensitive to polypeptides (polymyxin B), quinolones (including pipemidic, nalidixic, fleroxacin, lomefloxacin, ciprofloxacin, ofloxacin, norfloxacin, enrofloxacin), sulfonamides (sulfamethoxazole) and nitrofurans (including furazolidone). In β-lactam antibiotics, the strain showed resistance to cefoperazone, ceftizoxime, cefotaxime, ceftriaxone, ceftazidime, cefradine and oxacillin, while it was sensitive to penicillin, ampicillin, cefalexin and cefazolin. In tetracyclines antibiotics, the strain showed resistance to doxycycline, while it was sensitive to minocycline and tetracycline. Among other antibiotics, the strain showed resistance to rifampicin, while it was sensitive to novobiocin.

The results of Blast analysis in CARD database showed that 180 drug resistance genes belonging to 27 categories were found in the whole genome of the strain VSc190401 (Table 2). In terms of drug resistance phenotype and genotype correlation, the strain VSc190401 contained the streptomycin-resistant genes, *gidB* and *vatB* [35], and rifampin-resistant genes, *rpoB* [36]. The phenotype was consistent with the genotype. The novobiocin-resistant genes, *alaS* and *cysB* [37], nalidixic-resistant genes, *gyrA/B* and *parC/E* [38], tetracycline-resistant genes, *tet31/34/35/B/R/S/T* and *adeR* [39],

ciprofloxacin-resistant genes, *patA/B* [40], and bpolymyxin B-resistant genes, *PmrA/C/E*, *LpxA/C* and *rosB* [41], were found in the whole genome, while the strain was sensitive to these drugs. The phenotype was inconsistent with the genotype. In addition, the multiple resistance genes and complex genes of different antibiotics were also found in the strain, such as multiple resistance genes, *drrA* [42], *cpxA* and *ompR* [43], multidrug efflux pump systems, including ABC transporter superfamily of proteins *msbA* [44]; two-component signal transduction system, *EvgAS* [45]; two-component regulatory system, *BaeSR* [46]; an activator of *mtrCDE* multidrug-resistance efflux pump, *mtrA* [47]; MexEF-Opr multidrug efflux systems [48]; two-component regulatory systems, *VanRS* [49] and *ArlRS* [50]. These results showed that the resistance mechanism of the strain VSc190401 might be complicated. Phenotypes of multiple drug resistance without specific resistance genes suggested that there were multiple drug metabolism pathways. Supplementary Table 6 shows the annotation information of all drug resistance genes.

Table 2
The drug-resistance genes annotation of the strain VSc190401 in CARD databases

Drug resistance categories	Gene numbers	Drug resistance categories	Gene numbers
pleuromutilin antibiotic	3	penem	3
carbapenem	7	phenicol antibiotic	12
sulfonamide antibiotic	5	rifamycin antibiotic	4
aminoglycoside antibiotic	10	isoniazid	3
macrolide antibiotic	45	triclosan	11
glycopeptide antibiotic	4	acridine dye	10
tetracycline antibiotic	36	peptide antibiotic	14
monobactam	5	lincosamide antibiotic	1
diaminopyrimidine antibiotic	4	fluoroquinolone antibiotic	38
streptogramin antibiotic	5	nitroimidazole antibiotic	6
glycylcycline	5	penam	27
sulfone antibiotic	3	cephalosporin	10
aminocoumarin antibiotic	9	nybomycin	1
cephamycin	9		

3.7 Predictive analysis of pathogen-host interaction between the strain VSc190401 and host

According to annotation results of PHI database, the strain VSc190401 contained 518 genes related to pathogen-host interaction. Among them, there were 346 genes related to reduced virulence, 44 genes related to loss of pathogenicity, 36 genes related to hypervirulence, 12 genes related to lethal factors, 11

genes related to effector, three genes related to chemical resistance and two genes related to chemical sensitivity, and there were 108 genes with unaffected pathogenicity. The hypervirulence and effector genes were the key genes in correlation with pathogenicity. The hypervirulence of the strain VSc190401 included T3SS function genes, *esaN* and *GdpX1*, virulence regulatory factors, *MorA*, *ccpE*, *RsmA*, *raxP* and *CdpR* [51 – 54], two-component sensor kinase, *BfiS* [55], histidine kinase and response regulator two-component system, *TcrX/Y* [56], and iron ion transporters, *feoB* and *pchD*. The effector genes of the strain VSc190401 included T6SS components, *VgrG* and *clpV* [57], phospholipase D effector, *LpdA* [58], pleiotropic effector of virulence synthesis and pathogenicity attenuation, *RpiRc* [59]. Supplementary Table 7 lists the detailed annotation information of pathogen-host interaction genes.

4 Conclusions

The whole genome of pathogenic *V. scophthalmi* strain VSc190401 was 3,541,838 bp in length, including two circular chromosomes with the sizes of 3,286,294 bp and 202,664 bp, and two plasmids with the sizes of 24,538 bp and 28,342 bp, and this genome contained 3,185 coding genes. The result of gene functional annotation indicated that 2,648 genes were annotated into 22 types of genes in the COG database, accounting for 83.14% of total genes. Moreover, 2,298 genes were annotated into three classifications in the Blast2GO database, accounting for 72.15% of total genes. In addition, 1,915 genes were annotated into 196 known KEGG metabolic pathways, accounting for 60.13% of total genes. The analysis results based on VFDB database showed that the strain VSc190401 contained 334 potential virulence genes, including four secretion systems of T1SS, T2SS, T4SS, T6SS related genes and many different reported virulence genes. However, it only had complete T2SS secretion system. Blast results in CARD database showed that the strain contained 180 drug resistance genes belonging to 27 antibiotic resistance categories. However, many phenotypic resistance antibiotics were not related to drug resistance genes in the whole genome. Comparison analysis with PHI database obtained 809 genes related to pathogen-host interaction, including a variety of regulatory factors or regulatory systems, as well as T3SS and T6SS functional genes. Whole genome analysis suggested that pathogenic *V. scophthalmi* strain VSc190401 might have complex molecular mechanism of drug resistance and pathogenicity, which need to be further explored in-depth research.

Abbreviations

COG: Clusters of Orthologous Groups of proteins; GO: Gene Ontology; KEGG: Kyoto Encyclopedia of Genes and Genomes; VFDB: Virulence Factors of Pathogenic Bacteria; NR: Non-Redundant Protein Sequence Database in NCBI; PHI: Pathogen Host Interactions; CARD: Comprehensive Antibiotic Research Database; HGAP: hierarchical genomic assembly process; OLC: overlap layout consensus; CDSs: coding sequences; ANI: average nucleotide identity;

Declarations

Acknowledgements

Not applicable.

Authors’ contributions

Zheng Zhang: Isolated this strain, designed the research, performed antibiotic resistance phenotype experiment and phylogenetic analysis, wrote the draft; Yong-xiang Yu: Sequenced the whole genome and analyzed COG, GO, KEGG, and NR database; Yin-geng Wang: Examined the experimental design and polished the language; Xiao Liu and Lifang Wang: Performed the artificial infection experiment; Hao Zhang: Analyzed VFDB and PHI database; Mei-jie Liao: Analyzed CARD database; Bin Li: Participated in the artificial infection experiment. All authors read and approved the final manuscript.

Funding

This work was funded by National Key R&D Program of China (Grant:. 2019YFD0900104). Projects of International Exchange and Cooperation in Agriculture, Ministry of Agriculture and Rural Affairs of China-Science, Technology and Innovation Cooperation in Aquaculture with Tropical Countries along the Belt and Road. The project of Taishan industry leading talent (LJNY201802).

Availability of data and materials

The whole genome sequence of *Vibrio scophthalmi* strain VSc190401 has been deposited in the NCBI GenBank server under the SRA accession number PRJNA628013 for chromosome 1, chromosome 2, and the plasmids.

Ethics approval and consent to participate

Not applicable.

Consent for publication

All the authors agree to publish this paper.

Competing interests

The authors declare that they have no competing interests

References

1. Cerdag-Cuellar M, Rossello-Mora Ra, Lalucat J, Jofre J, Blanch A. *Vibrio scophthalmi* sp. nov., a New Species from Turbot (*Scophthalmus maximus*). Int J Syst Bacteriol. 1997;47:58–61. https://doi.org/10.1099/00207713-47-1-58.
2. Sawabe T, Kita-Tsukamoto K, Thompson FL. Inferring the Evolutionary History of Vibrios by Means of Multilocus Sequence Analysis. J Bacteriol. 2007;189:7932–6. https://doi.org/10.1128/JB.00693-07.
3. Tarazona E, Pérez-Cataluña A, Lucena T, Arahal DR, Macián MC, Pujalte MJ. Multilocus Sequence Analysis of the redefined clade Scophthalmi in the genus *Vibrio*. Syst Appl Microbiol. 2015;38:169–75. https://doi.org/10.1016/j.syapm.2015.03.005.
4. Blanch AR, Alsina M, Simón M, Jofre J. Determination of bacteria associated with reared turbot (*Scophthalmus maximus*) larvae. J Appl Microbiol. 1997;82:729–34. https://doi.org/10.1046/j.1365-2672.1997.00190.x.
5. Qiao G, Lee DC, Woo SH, Li H, Xu D-H, Park S Il. Microbiological characteristics of *Vibrio scophthalmi* isolates from diseased olive flounder *Paralichthys olivaceus*. Fish Sci. 2012;78:853–63. https://doi.org/10.1007/s12562-012-0502-8.
6. Soffientino B, Gwaltney T, Nelson D, Specker J, Mauel M, Gómez-Chiarri M. Infectious necrotizing enteritis and mortality caused by *Vibrio carchariae* in summer flounder *Paralichthys dentatus* during intensive culture. Dis Aquat Organ. 1999;38:201–10. https://doi.org/10.3354/dao038201.
7. Sitjà-Bobadilla A, Pujalte MJ, Bermejo A, Garay E, Alvarez-Pellitero P, Pérez-Sánchez J. Bacteria associated with winter mortalities in laboratory-reared common dentex (*Dentex dentex* L.). Aquac Res. 2007;38:733–9. https://doi.org/10.1111/j.1365-2109.2007.01719.x.
8. Beaz Hidalgo R, Cleenwerck I, Balboa S, De Wachter M, Thompson FL, Swings J, et al. Diversity of Vibrios associated with reared clams in Galicia (NW Spain). Syst Appl Microbiol. 2008;31:215–22. https://doi.org/10.1016/j.syapm.2008.04.001.
9. Valdenegro-Vega V, Naeem S, Carson J, Bowman JP, Tejedor del Real JL, Nowak B. Culturable microbiota of ranched southern bluefin tuna (*Thunnus maccoyii* Castelnau). J Appl Microbiol. 2013;:n/a-n/a. https://doi.org/10.1111/jam.12286.
10. Lee N-S, Kim D-J, Lee B-I, Kim SK, Kim MS, Kim YC. *Vibrio scophthalmi* infection in Japanese eel *Anguilla japonica* during seawater adaption. J fish Pathol. 2012;25:173–80. https://doi.org/10.7847/jfp.2012.25.3.173.
11. Kang BJ. A study on the characteristics of bacteria isolated from cultured flouders *Paralichthys olivaceus* showing disease symptoms in Jeju area of Korea. CheJu National University; 2003. (in Korean with English abstract)
12. Zheng Z. Epizootic Investigation and Aetiological study on the Bacterial Diseases in Cultured Turbot (*Scophthalmus maximus*). Ocean University of China; 2004. (in Chinese with English abstract)

13. Thompson FL, Gevers D, Thompson CC, Dawyndt P, Naser S, Hoste B, et al. Phylogeny and Molecular Identification of Vibrios on the Basis of Multilocus Sequence Analysis. Appl Environ Microbiol. 2005;71:5107–15. https://doi.org/10.1128/AEM.71.9.5107-5115.2005.
14. Montero AB, Austin B. Characterization of extracellular products from an isolate of *Vibrio harveyi* recovered from diseased post-larval *Penaeus vannamei* (Bonne). J Fish Dis. 1999;22:377–86. https://doi.org/10.1046/j.1365-2761.1999.00189.x.
15. Qiao G, Jang I-K, Won KM, Woo SH, Xu D-H, Park S Il. Pathogenicity comparison of high- and low-virulence strains of *Vibrio scophthalmi* in olive flounder *Paralichthys olivaceus*. Fish Sci. 2013;79:99–109. https://doi.org/10.1007/s12562-012-0567-4.
16. Cui Huijing, Meng Yuxia, Feng Wenqian, Zhao Qiancheng MY. Identification and antimicrobial susceptibility test of *Vibrio scophthalmi* isolated from the intestine of cultured turbot *Scophthalmus maximus*. Fish Sci. 2017;36:125–31.(in Chinese with English abstract)
17. Wang lan, Wang Yingeng, Zhang Zheng, Chen Guohua, Liao Meijie, Chen Xia GW. Diversity and drug resistance of bacterial pathogens isolated from bacterial ascetic disease in cultured turbot *Scophthalmus maximus*. Prog Fish Sci. 2017;38:17–24. (in Chinese with English abstract)
18. Chin C-S, Alexander DH, Marks P, Klammer AA, Drake J, Heiner C, et al. Nonhybrid, finished microbial genome assemblies from long-read SMRT sequencing data. Nat Methods. 2013;10:563–9. https://doi.org/10.1038/nmeth.2474.
19. Myers EW. A whole-genome assembly of *Drosophila*. Science. 2000;287:2196–204. https://doi.org/10.1126/science.287.5461.2196.
20. Tarailo-Graovac M, Chen N. Using repeatmasker to identify repetitive elements in genomic sequences. Curr Protoc Bioinforma. 2009;25:4.10.1-4.10.14. https://doi.org/10.1002/0471250953.bi0410s25.
21. Lagesen K, Hallin P, Rødland EA, Stærfeldt H-H, Rognes T, Ussery DW. RNAmmer: consistent and rapid annotation of ribosomal RNA genes. Nucleic Acids Res. 2007;35:3100–8. https://doi.org/10.1093/nar/gkm160.
22. Lowe TM, Eddy SR. tRNAscan-SE: A program for improved detection of transfer rna genes in genomic sequence. Nucleic Acids Res. 1997;25:955–64. https://doi.org/10.1093/nar/25.5.955.
23. Cai S, Cheng H, Pang H, Jian J, Wu Z. AcfA is an essential regulator for pathogenesis of fish pathogen *Vibrio alginolyticus*. Vet Microbiol. 2018;213:35–41. https://doi.org/10.1016/j.vetmic.2017.11.016.
24. Kim H, Bhunia AK. Secreted *Listeria* adhesion protein (Lap) influences Lap-mediated *Listeria monocytogenes* paracellular translocation through epithelial barrier. Gut Pathog. 2013;5:16. https://doi.org/10.1186/1757-4749-5-16.
25. Glaser P, Sakamoto H, Bellalou J, Ullmann A, Danchin A. Secretion of cyclolysin, the calmodulin-sensitive adenylate cyclase-haemolysin bifunctional protein of Bordetella pertussis. EMBO J. 1988;7:3997–4004. https://doi.org/10.1002/j.1460-2075.1988.tb03288.x.

26. Salter SJ, Hinds J, Gould KA, Lambertsen L, Hanage WP, Antonio M, et al. Variation at the capsule locus, *cps*, of mistyped and non-typable *Streptococcus pneumoniae* isolates. Microbiology. 2012;158:1560–9. https://doi.org/10.1099/mic.0.056580-0.
27. Waite RD, Penfold DW, Struthers JK, Dowson CG. Spontaneous sequence duplications within capsule genes *cap8E* and tts control phase variation in *Streptococcus pneumoniae* serotypes 8 and 37. Microbiology. 2003;149:497–504. https://doi.org/10.1099/mic.0.26011-0.
28. Núñez C, León R, Guzmán J, Espín G, Soberón-Chávez G. Role of *Azotobacter vinelandii mucA* and *mucC* gene products in alginate production. J Bacteriol. 2000;182:6550–6. https://doi.org/10.1128/JB.182.23.6550-6556.2000.
29. Jie G. Screening of alginate lyase producing strain and cloning and expression of its gene. Dalian University of Technology; 2018. (in Chinese with English abstract)
30. Mashruwala AA, Eilers BJ, Fuchs AL, Norambuena J, Earle CA, van de Guchte A, et al. The ClpCP complex modulates respiratory metabolism in *Staphylococcus aureus* and is regulated in a SrrAB-dependent manner. J Bacteriol. 2019;201. https://doi.org/10.1128/JB.00188-19.
31. Robey M, Cianciotto NP. *Legionella pneumophila feoAB* promotes ferrous iron uptake and intracellular infection. Infect Immun. 2002;70:5659–69. https://doi.org/10.1128/IAI.70.10.5659-5669.2002.
32. Adhikari P, Berish SA, Nowalk AJ, Veraldi KL, Morse SA, Mietzner TA. The *fbpABC* locus of *Neisseria gonorrhoeae* functions in the periplasm-to-cytosol transport of iron. J Bacteriol. 1996;178:2145–9. https://doi.org/10.1128/JB.178.7.2145-2149.1996.
33. Haralalka S, Nandi S, Bhadra RK. Mutation in the *relA* Gene of *Vibrio cholerae* affects in vitro and in vivo expression of virulence factors. J Bacteriol. 2003;185:4672–82. https://doi.org/10.1128/JB.185.16.4672-4682.2003.
34. Wei C, Ding T, Chang C, Yu C, Li X, Liu Q. Global regulator PhoP is necessary for motility, biofilm formation, exoenzyme production, and virulence of *Xanthomonas citri* subsp. *citri* on citrus plants. Genes. 2019;10:340. https://doi.org/10.3390/genes10050340.
35. Smittipat N, Juthayothin T, Billamas P, Jaitrong S, Rukseree K, Dokladda K, et al. Mutations in *rrs*, *rpsL* and *gidB* in streptomycin-resistant *Mycobacterium tuberculosis* isolates from Thailand. J Glob Antimicrob Resist. 2016;4:5–10. https://doi.org/10.1016/j.jgar.2015.11.009.
36. Zaw MT, Emran NA, Lin Z. Mutations inside rifampicin-resistance determining region of *rpoB* gene associated with rifampicin-resistance in *Mycobacterium tuberculosis*. J Infect Public Health. 2018;11:605–10. https://doi.org/10.1016/j.jiph.2018.04.005.
37. Jovanovic M, Lilic M, Janjusevic R, Jovanovic G, Savic DJ, Milija J. tRNA synthetase mutants of *Escherichia coli* K-12 are resistant to the gyrase inhibitor novobiocin. J Bacteriol. 1999;181:2979–83. http://www.ncbi.nlm.nih.gov/pubmed/10217798.
38. Bae D, Baek H, Jeong S, Lee Y. Amino acid substitutions in *gyrA* and *parC* associated with quinolone resistance in nalidixic acid-resistant *Salmonella isolates*. Ir Vet J. 2013;66:23. https://doi.org/10.1186/2046-0481-66-23.

39. Costello SE, Gales AC, Morfin-Otero R, Jones RN, Castanheira M. Mechanisms of resistance, clonal expansion, and increasing prevalence of *Acinetobacter baumannii* strains displaying elevated tigecycline MIC values in Latin America. Microb Drug Resist. 2016;22:253–8. https://doi.org/10.1089/mdr.2015.0168.
40. Lupien A, Billal DS, Fani F, Soualhine H, Zhanel GG, Leprohon P, et al. Genomic characterization of ciprofloxacin resistance in a laboratory-derived mutant and a clinical isolate of *Streptococcus pneumoniae*. Antimicrob Agents Chemother. 2013;57:4911–9. https://doi.org/10.1128/AAC.00418-13.
41. Zhang W, Aurosree B, Gopalakrishnan B, Balada-Llasat J-M, Pancholi V, Pancholi P. The role of *LpxA/C/D* and *pmrA/B* gene systems in colistin-resistant clinical strains of *Acinetobacter baumannii*. Front Lab Med. 2017;1:86–91. https://doi.org/10.1016/j.flm.2017.07.001.
42. Kardan-Yamchi J, Kazemian H, Haeili M, Harati AA, Amini S, Feizabadi MM. Expression analysis of 10 efflux pump genes in multidrug-resistant and extensively drug-resistant *Mycobacterium tuberculosis* clinical isolates. J Glob Antimicrob Resist. 2019;17:201–8. https://doi.org/10.1016/j.jgar.2019.01.003.
43. Lin X, Wang C, Guo C, Tian Y, Li H, Peng X. Differential regulation of OmpC and OmpF by AtpB in *Escherichia coli* exposed to nalidixic acid and chlortetracycline. J Proteomics. 2012;75:5898–910. https://doi.org/10.1016/j.jprot.2012.08.016.
44. Chiu H-C, Lin T-L, Yang J-C, Wang J-T. Synergistic effect of *imp/ostA* and *msbA* in hydrophobic drug resistance of *Helicobacter pylori*. BMC Microbiol. 2009;9:136. https://doi.org/10.1186/1471-2180-9-136.
45. Eguchi Y, Oshima T, Mori H, Aono R, Yamamoto K, Ishihama A, et al. Transcriptional regulation of drug efflux genes by EvgAS, a two-component system in *Escherichia coli*. Microbiology. 2003;149:2819–28. https://doi.org/10.1099/mic.0.26460-0.
46. Baranova N, Nikaido H. The BaeSR two-component regulatory system activates transcription of the *yegMNOB* (*mdtABCD*) transporter gene cluster in *Escherichia coli* and increases its resistance to novobiocin and deoxycholate. J Bacteriol. 2002;184:4168–76. https://doi.org/10.1128/JB.184.15.4168-4176.2002.
47. Warner DM, Folster JP, Shafer WM, Jerse AE. Regulation of the MtrC-MtrD-MtrE efflux-pump system modulates the in vivo fitness of *Neisseria gonorrhoeae*. J Infect Dis. 2007;196:1804–12. https://doi.org/10.1086/522964.
48. Sobel ML, Neshat S, Poole K. Mutations in PA2491 (*mexS*) Promote MexT-Dependent *mexEF-oprN* expression and multidrug resistance in a clinical strain of *Pseudomonas aeruginosa*. J Bacteriol. 2005;187:1246–53. https://doi.org/10.1128/JB.187.4.1246-1253.2005.
49. Silva JC, Haldimann A, Prahalad MK, Walsh CT, Wanner BL. In vivo characterization of the type A and B vancomycin-resistant enterococci (VRE) VanRS two-component systems in *Escherichia coli*: A nonpathogenic model for studying the VRE signal transduction pathways. Proc Natl Acad Sci. 1998;95:11951–6. https://doi.org/10.1073/pnas.95.20.11951.

50. Memmi G, Nair DR, Cheung A. Role of ArlRS in autolysis in methicillin-sensitive and methicillin-resistant *Staphylococcus aureus* strains. J Bacteriol. 2012;194:759–67. https://doi.org/10.1128/JB.06261-11.
51. Phippen CW, Mikolajek H, Schlaefli HG, Keevil CW, Webb JS, Tews I. Formation and dimerization of the phosphodiesterase active site of the *Pseudomonas aeruginosa* MorA, a bi-functional c-di-GMP regulator. FEBS Lett. 2014;588:4631–6. https://doi.org/10.1016/j.febslet.2014.11.002.
52. Hartmann T, Baronian G, Nippe N, Voss M, Schulthess B, Wolz C, et al. The catabolite control protein E (CcpE) affects virulence determinant production and pathogenesis of *Staphylococcus aureus*. J Biol Chem. 2014;289:29701–11. https://doi.org/10.1074/jbc.M114.584979.
53. Zhao J, Yu X, Zhu M, Kang H, Ma J, Wu M, et al. Structural and Molecular Mechanism of CdpR Involved in Quorum-Sensing and Bacterial Virulence in Pseudomonas aeruginosa. PLOS Biol. 2016;14:e1002449. https://doi.org/10.1371/journal.pbio.1002449.
54. Shen Y, Sharma P, Silva FG da, Ronald P. The Xanthomonas oryzae pv. oryzae raxP and raxQ genes encode an ATP sulphurylase and adenosine-5'-phosphosulphate kinase that are required for AvrXa21 avirulence activity. Mol Microbiol. 2002;44:37–48. https://doi.org/10.1046/j.1365-2958.2002.02862.x.
55. Pletzer D, Mansour SC, Wuerth K, Rahanjam N, Hancock REW. New mouse model for chronic infections by gram-negative bacteria enabling the study of anti-infective efficacy and host-microbe interactions. MBio. 2017;8. https://doi.org/10.1128/mBio.00140-17.
56. Bhattacharya M, Das AK. Inverted repeats in the promoter as an autoregulatory sequence for TcrX in *Mycobacterium tuberculosis*. Biochem Biophys Res Commun. 2011;415:17–23. https://doi.org/10.1016/j.bbrc.2011.09.143.
57. Hachani A, Lossi NS, Hamilton A, Jones C, Bleves S, Albesa-Jové D, et al. Type VI secretion system in *Pseudomonas aeruginosa*. J Biol Chem. 2011;286:12317–27. https://doi.org/10.1074/jbc.M110.193045.
58. Schroeder GN, Aurass P, Oates C V., Tate EW, Hartland EL, Flieger A, et al. *Legionella pneumophila* effector LpdA is a palmitoylated phospholipase D virulence factor. Infect Immun. 2015;83:3989–4002. https://doi.org/10.1128/IAI.00785-15.
59. Gaupp R, Wirf J, Wonnenberg B, Biegel T, Eisenbeis J, Graham J, et al. RpiRc is a pleiotropic effector of virulence determinant synthesis and attenuates pathogenicity in *Staphylococcus aureus*. Infect Immun. 2016;84:2031–41. https://doi.org/10.1128/IAI.00285-16.

Figures

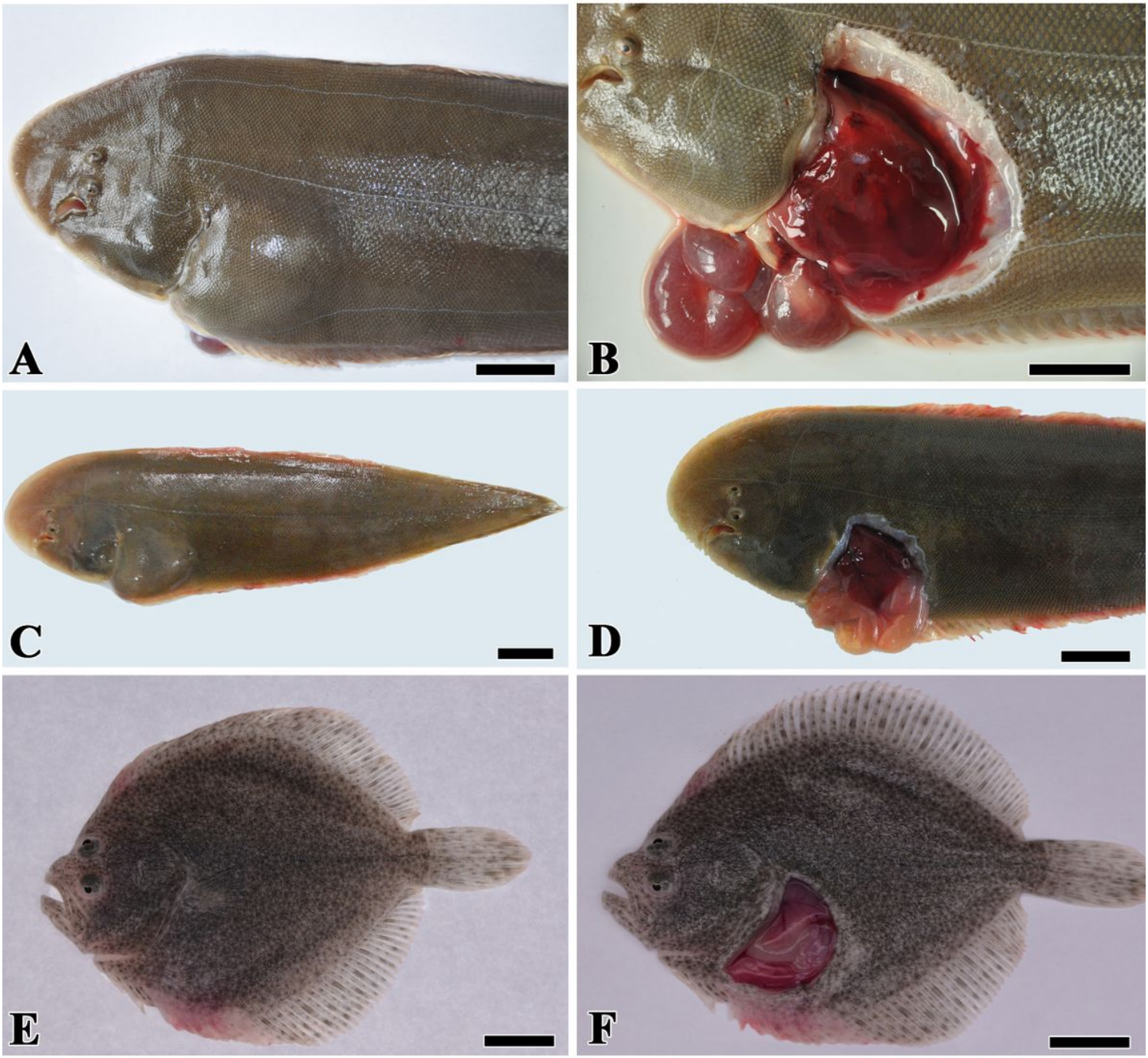

Figure 1

The symptoms of diseased fish with natural infection and artificial infection V. scophthalmi strain VSc190401. A: Naturally infected half-smooth tongue sole had obvious abdominal lump. B: Naturally infected half-smooth tongue sole showed serious internal organ hyperemia and enteritis. C: Artificially infected half-smooth tongue soles showed the same symptoms of abdominal limp. D: Artificially infected half-smooth tongue soles appeared same internal organ lesions as naturally infected case. E: Artificially infected turbot did not appear abdominal lump. F: Artificially infected turbot showed serious organ hyperemia and enteritis. Bar = 2 cm.

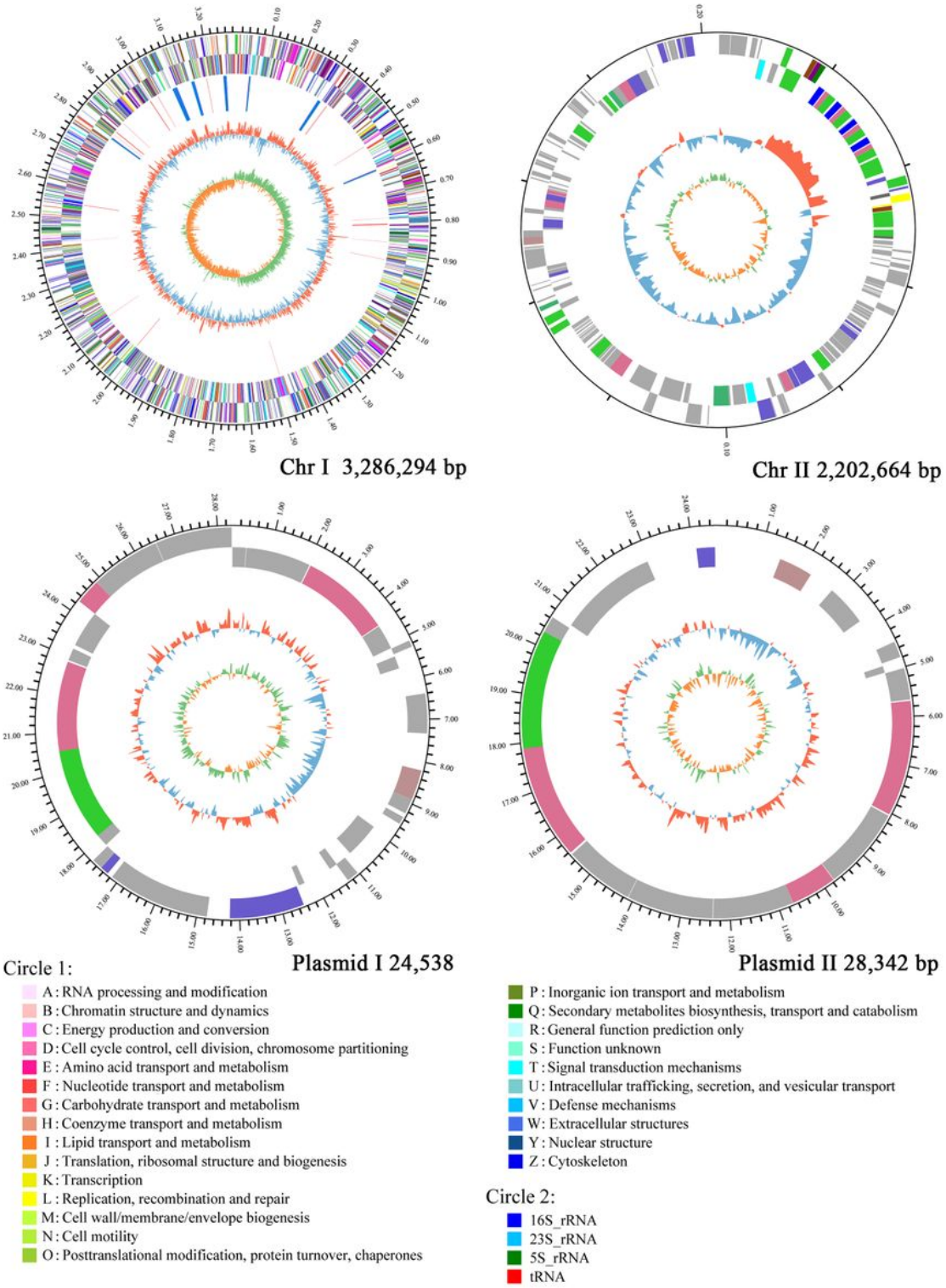

Figure 2

Circular genome maps of V. scophthalmi strain VSc190401

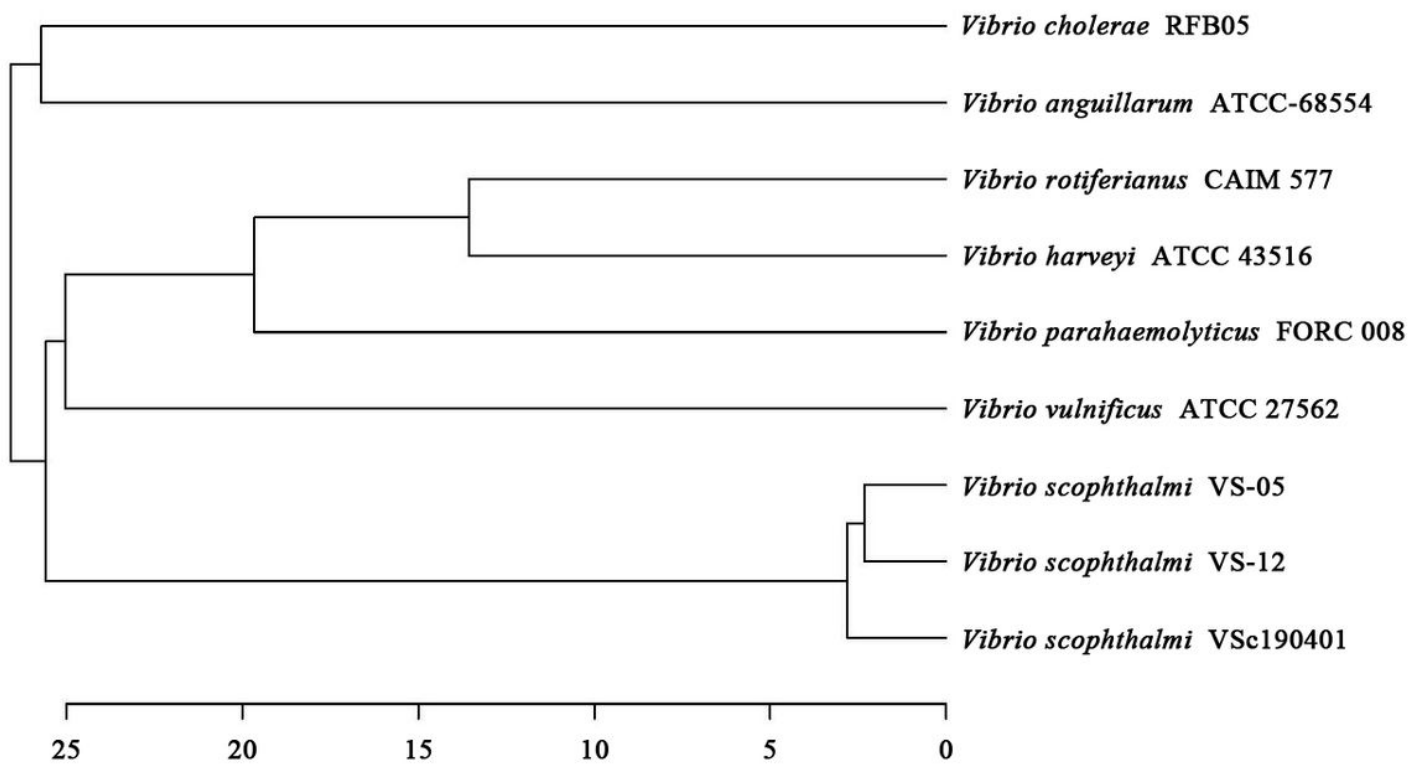

Figure 3

Phylogenetic tree analysis based on ANI values of V. scophthalmi strain VSc190401 and the complete genomes of eight bacterial strains downloaded from NCBI database. The scale represents genetic distance.

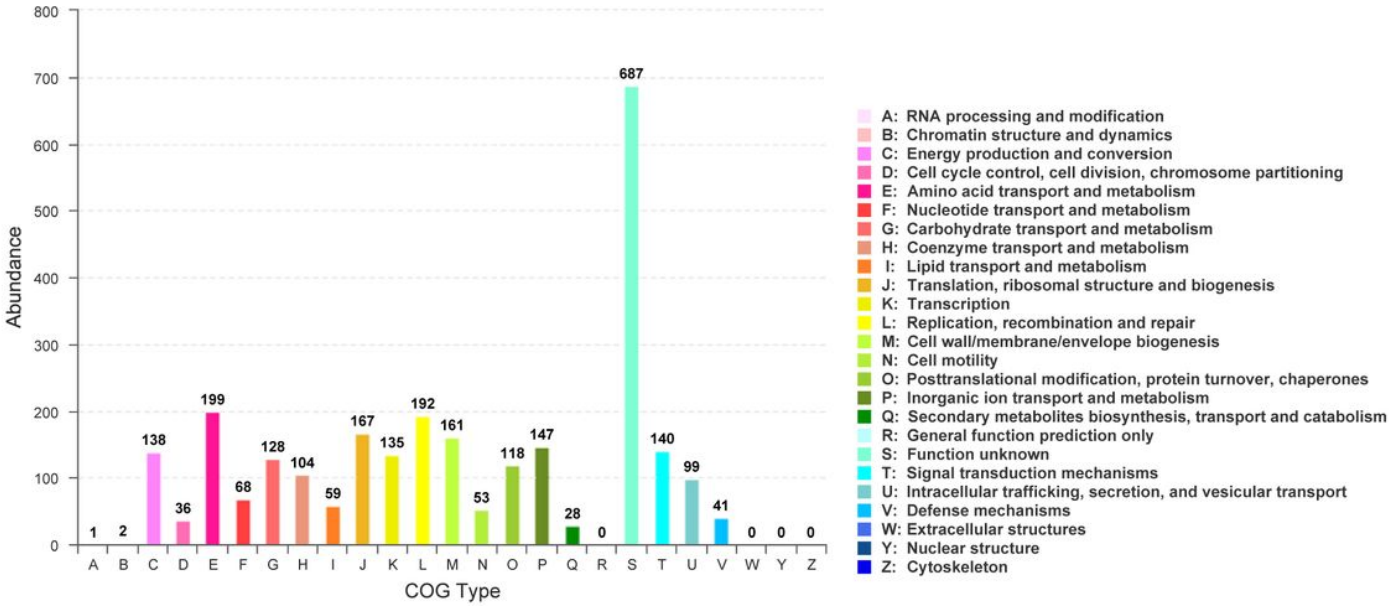

Figure 4

COG functional annotation of CODs in the whole genome of V. scophthalmi strain VSc190401.

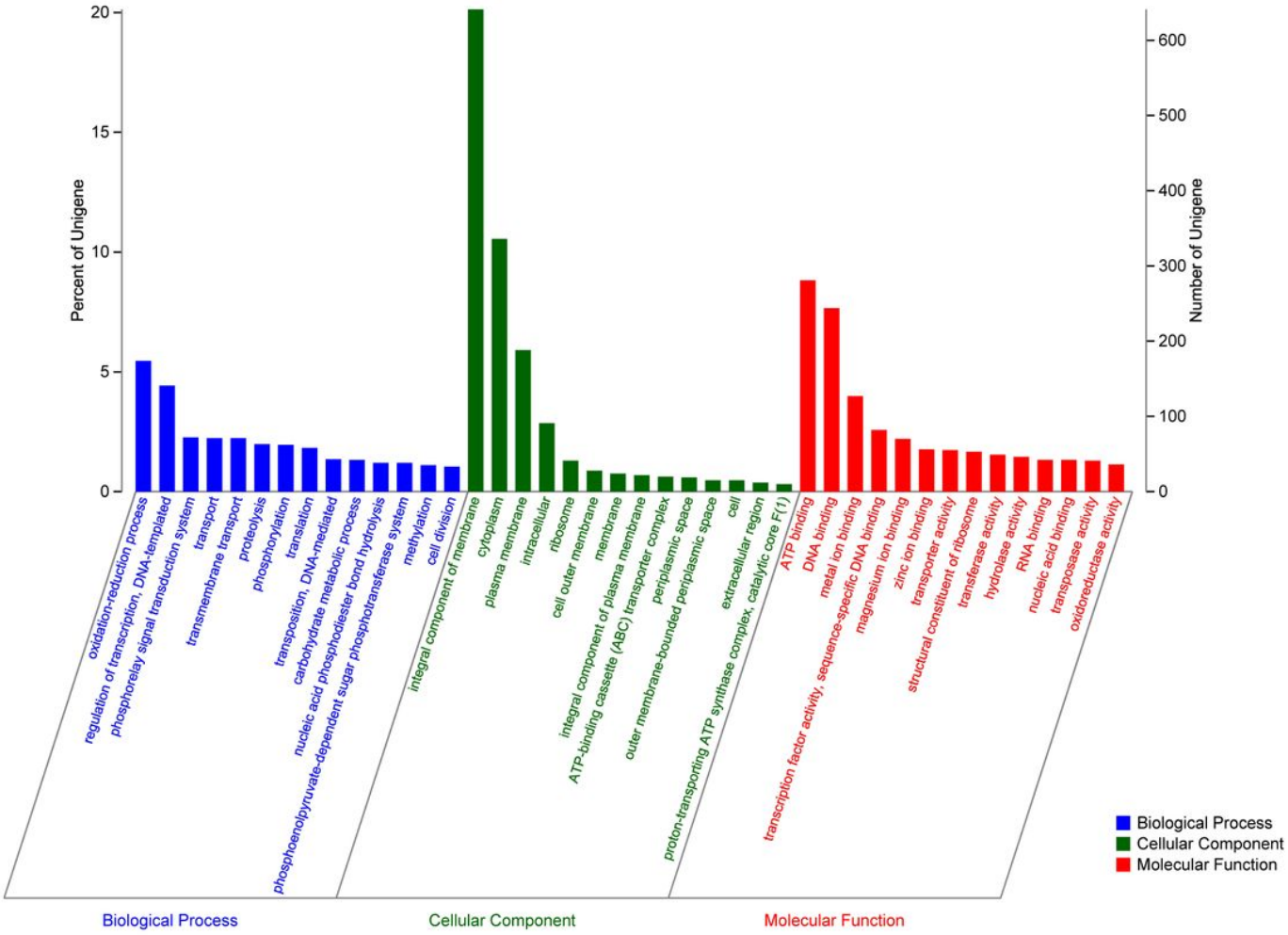

Figure 5

GO functional annotation of CODs in the whole genome of V. scophthalmi strain VSc190401.

Figure 6

The KEGG pathway annotation results of V. scophthalmi strain VSc190401. The ordinate indicates the level 2 KEGG pathway classification, and the abscissa indicates the number of genes under the annotation of this classification. Different column colors represent the level 1 KEGG pathway classification. The rightmost bar indicates the number of genes under different level 1 classifications. Since the same gene may be annotated into multiple level 2 classifications, the number of genes classified by level 1 will be de-redundant.

Supplementary Files

This is a list of supplementary files associated with this preprint. Click to download.

- SupplementaryTable3TheKEGGpathwayannotation.xls
- SupplementaryFigure1Genomeislandslinearmap.jpg
- SupplementaryTable4Thegenomicislandsonchromosomel.xls
- SupplementaryTable5Thevirulencefactorsannotation.xls
- SupplementaryTable6Thedrugresistancegenesannotation.xls
- SupplementaryTable7ThePHIgenesannotation.xls
- SupplementaryTable1TheCOGfunctionalannotation.xls
- SupplementaryTable2TheGOfunctionalannotation.xls
- SupplementaryFigure2Thesecretorysystempathway.jpg